Advances in Science and Technology Research Journal

Advances in Science and Technology Research Journal 2023, 17(6), 274–287
https://doi.org/10.12913/22998624/172365
ISSN 2299-8624, License CC-BY 4.0

Received: 2023.06.12
Accepted: 2023.09.15
Published: 2023.11.21

The Possibility of Using the Finite Element Method for Determining Thermal Diffusivity on the Example of Nickel Using the Classic and the Modified Pulse Method

Robert Szczepaniak[1*], Janusz Terpiłowski[2], Grzegorz Woroniak[3]

[1] Polish Air Force University, Dywizjonu 303, No. 35, 08-521 Dęblin, Poland
[2] Military University of Technology, Sylwestra Kaliskiego 2, 00-908 Warsaw, Poland
[3] Bialystok University of Technology, Wiejska 45A, 15-351 Bialystok, Poland
* Corresponding author's email: r.szczepaniak@law.mil.pl

ABSTRACT

The main purpose of the work was to present the possibility of using the finite element method implemented in the COMSOL 3.5a software in the heat transfer symmetry 2D module to determine thermal diffusivity by using the classic and modified pulse methods. The method of determining the thermal diffusivity by means of measuring and recording the course of the temperature difference between the extreme surfaces of the tested sample and changes in the temperature increase on the back surface after a laser shot at its front surface, assuming that the sample is adiabatic for a representative experimental course at a given temperature, was discussed. This paper presents the basic metrological conditions for the implementation of the modified pulse method for testing the temperature characteristics of thermal diffusivity on the example of nickel. The heat pulse generated by using the laser method at the extreme surface of the sample for a thermostatic temperature of 341.8 °C was simulated. Using the inverse problem in both the classic and modified methods, the thermal diffusivity of the material in question was determined and these results were compared with the experimentally obtained values. The values of thermal diffusivity differ from those obtained experimentally by 3.3% for the classic method and approximately 2.5% for the modified method. A preliminary analysis of the influence of the number of nodal points on the numerical results obtained was also carried out and the results for the number of nodes between 64 and 17,000 change by only 1.1%. The paper presents a combination of experimental and numerical studies which is useful in science and simplifies the process of time-consuming experimental studies.

Keywords: thermal diffusivity, FEM, heat exchange, flash method.

INTRODUCTION

The determination of thermal diffusivity is a crucial aspect in the field of materials science and engineering. It is a key parameter for analyzing the heat transfer characteristics of a material and is essential in the design of heat transfer systems. Various methods have been proposed for determining thermal diffusivity, including the laser flash, transient plane source, and pulse methods. However, due to its accuracy and efficiency, the finite element method has recently emerged as a promising approach for determining thermal diffusivity. In this paper, the possibility of using the finite element method to determine thermal diffusivity using both the classic and modified pulse methods was investigated. The classic pulse method involves heating the surface of a material with a short pulse of energy and monitoring the temperature response at a nearby point. The modified pulse method involves applying a longer pulse of energy to the surface of the material and monitoring the temperature response at various points. Both methods are widely used for measuring thermal diffusivity, but the modified pulse method has been shown to provide more

accurate results [1]. The authors focused on the example of nickel to demonstrate the feasibility of using the finite element method with the classic and modified pulse methods. Nickel is an important material in many industries, including aerospace, electronics, and automotive, and its thermal properties have been extensively studied. In recent years, the finite element method has gained increasing attention as a promising approach for determining thermal diffusivity in materials [2, 3]. This method involves solving the heat diffusion equation using numerical simulations, which can provide accurate and efficient results. The use of the finite element method for determining thermal diffusivity has been investigated for a wide range of materials, including metals, ceramics, and polymers. COMSOL Multiphysics software is very frequently used for calculations in the area of heat transfer, as well as for the multi-physics simulation platform [4-6]. It is popular for heat transfer calculations in thin-film structures [7-9]. The influence of waviness is of great importance for calculations of heat transfer phenomena in thin films and in complex flow models used, among others, in aviation technology, e.g., rocket nozzles [10], engines [11] as well as in its heat conduction in microchannel flows [12], and heat exchangers [13, 14] which is a frequently tackled problem of modern mechanical engineering. In the case of heat transfer studies based on determining the global temperature distribution on the surface, it is necessary to take into account the thermal properties of all layers in the analysis [15], in particular, if the thickness is a square function, as in the case of determining thermal diffusivity using the laser flash method (LFA –Laser Flash Analysis), where the thickness is given to the second power [16].

Several studies have investigated the use of the finite element method to determine thermal diffusivity in materials [17-19].

For instance, Kuk-Hee Lim et al. [20], to minimize the error of the flash method in the measurement of thermal diffusivity of a thin sample covered with graphite, proposed a 3-layer model that takes into account the corrections of the finite pulse effect and the heat loss effect. It was found that the proposed three-layer model significantly reduces the measurement error. In their study, [21] Philipp et al. checked the accuracy limitations of laser flash analysis due to its underlying computational framework. To this end, they developed an exceptionally accurate and comprehensive computational framework and applied it to the data from simulation experiments. They quantified the impact of different (simulated) test conditions on the accuracy of the results by comparing the fit of their calculation framework with the simulated input parameters. In another study, Ruffio et al. [22] investigated the 3D flash method and argued that estimating the thermal diffusivity of homogeneous orthotropic materials is practical and efficient. The experimental setup is based on infrared thermography and thermal pulse excitation. A corresponding model is derived and solved analytically. The unknown parameters are then estimated using an estimator that combines measurements and model outputs. Their work, however, was only numerical. Malinaric et al. [23] studied the influence of heat source power and design on the accuracy of thermophysical parameters measurements in several transitional methods. The credibility of the analytical model of the Transient Plane Source method was confirmed by them by comparing it with the numerical model obtained by the finite element method (FEM), which uses three models of the material composition of the heat source. Temperature functions are determined based on numerical answers obtained by the FEM method and the analytical solution. Icing is a serious problem affecting the aviation sector, which is forced to use anti-icing and anti-icing systems to ensure the safety of flights. Garcia et al. [24] investigated the effect of the thermal properties of various materials on the temperature distribution obtained from a heater operating at anti-icing temperatures (5–10 °C) during a short on-time step. The authors note that the thermal diffusivity of the various layers that make up the systems must be considered an important design factor. The many parameters and the need to test the systems under real icing conditions or at least under forced convection conditions would result in very complex test matrices. In addition, experimental conditions are not easily reproduced in the laboratory, and wind tunnel testing under icing conditions is expensive. Garcia et al. [24] used the commercial Code Aster solver software with space-time discretization to calculate temperatures as a time and sample position function. Time discretization was performed using the finite difference method, and spatial discretization was performed using both 3D and 2D FEM models. Beaufait et al. [25] studied a method of measuring thermal diffusivity for samples of arbitrary geometry and unknown material properties. The aim was to fit the thermal diffusivity curve

using numerical simulation and measuring the transition temperature inside the tested object. This approach is designed to evaluate the material properties of a bulk object that has the structure of a composite material, such as underground soil. The method creates the boundary conditions necessary to apply the analytical theory found in the literature. The authors found that the measurements correlate best with theory and simulation, performed with COMSOL Multiphysics software, at positions between the center and the surface of the object. In conclusion, the use of the finite element method for determining thermal diffusivity using the classic and modified pulse methods has been investigated in several studies. These studies have demonstrated the accuracy and efficiency of the finite element method for determining thermal diffusivity in a wide range of materials, including metals, polymers, and composites. The use of the finite element method for determining thermal diffusivity has the potential to contribute to the development of more accurate and efficient methods for analyzing the thermal properties of materials. Overall, this paper aimed to provide a comprehensive analysis of the feasibility of using the finite element method for determining thermal diffusivity using the classic and modified pulse methods, with a focus on nickel as an example material. The results of this study have the potential to contribute to the development of more accurate and efficient methods for analyzing the thermal properties of materials.

Many nickel-based alloys are used in the aerospace industry, which is why the presented research was conducted on this material. Nickel alloys for the aerospace industry are selected based on their resistance to extreme heat, corrosion and continuous wear, as well as their magnetic properties. Nickel alloys are one of the most durable materials in terms of construction; they are also characterized by good electrical conductivity. During the experimental studies, an attempt was also made to identify Curie points in ferromagnetic materials –a clear phase transition of the second kind. Therefore, nickel was selected as a test material with a low phase transition temperature.

METHOD FOR DETERMINING THE THERMAL DIFFUSIVITY OF SOLIDS

The boundary conditions in the heat transfer model, based on which the thermal diffusivity is determined by using this pulse method [26], are shown in Figure 1. They are identical to the classic Parker method [27]:

$$\Theta(x,0) = \begin{cases} = \dfrac{Q}{\rho c_p g}, dla\ 0 \le x \le g \\ = 0, dla\ g < x \le l \end{cases} \quad (1)$$

where: $\Theta\ (x,\ 0) = T(x,\ 0) - T_0$ – the initial distribution of the excess temperature in the sample, where T_0 is the constant temperature of the sample just prior to the creation of a rectangular temperature pulse;
g – thickness of the layer in the sample in which a rectangular temperature pulse is generated by a heat source with surface density Q;
Q – heat source with surface density.

The general solution of the unsteady heat conduction equation given in the monograph by Carslaw and Jaeger [29]:

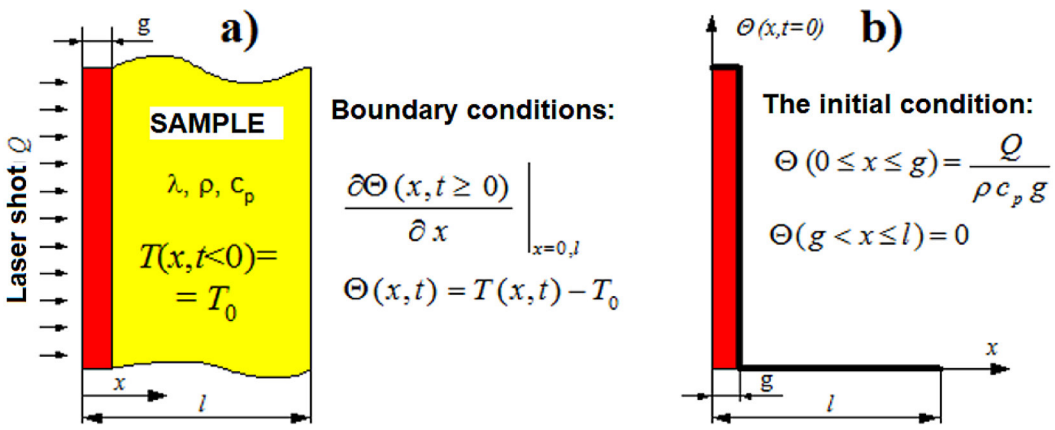

Fig. 1. Heat transfer model used for thermal diffusivity of solids determined with the classic and the modified pulse methods [28]

$$a\frac{\partial^2\Theta(\tau,x)}{\partial x^2}=\frac{\partial\Theta(\tau,x)}{\partial t} \tag{2}$$

where: a – thermal diffusivity;
t – time.

In a one-dimensional and adiabatic sample with initial condition $\Theta(x, 0)$, has the following form:

$$\Theta(x,t)=\frac{1}{l}\int_0^l\Theta(x',0)dx'+\frac{2}{l}\sum_{n=1}^{\infty}exp\left(-\frac{n^2\pi^2}{l^2}at\right)cos\frac{n\pi x}{l}\int_0^l\Theta(x',0)\,cos\frac{n\pi x'}{l}dx' \tag{3}$$

and after taking into account the initial condition (1) and the inequality $g \ll l$, they can be written in the following form:

$$\Theta(x,t)=\Theta_\infty\left[1+2\sum_{n=1}^{\infty}cos\left(\frac{n\pi x}{l}\right)\exp\left(-n^2\frac{t}{\tau}\right)\right] \tag{4}$$

where: τ – characteristic time is given by the following relation:

$$\tau=\frac{l^2}{\pi^2 a} \tag{5}$$

Θ_∞ – is the average value of the excess temperature of the sample after the cessation of the transient process caused by the surface heat source of surface density Q and is equal to:

$$\Theta_\infty=\Theta(\mathrm{x=l,t=\infty})=\frac{\mathrm{Q}}{\rho\mathrm{c_p l}} \tag{6}$$

At the same time, solution (4) is correct assuming that $g \ll l$.

The classic pulse method for determining thermal diffusivity (Parker method)

In the classic Parker method, thermal diffusivity is expressed by the following formula:

$$a=\frac{1.368\,l^2}{\pi^2 t_{0,5}} \tag{7}$$

where: $t_{0,5}$ – is the so-called half time, which corresponds to the time after which the excess temperature of the back surface of the sample wall reaches half of its maximum value.

Another way of determining the thermal diffusivity in the classic Parker method is to extrapolate the linear segment of the excess temperature growth curve $\Theta'(x, t) = \Theta(l, t)$ to the intersection with the t axis. Then, after t_x denotes the time corresponding to the intersection point of the linear section of the curve $\Theta'(x, t)$ with the t axis, we obtain:

$$a=\frac{0.48\,l^2}{\pi^2 t_x} \tag{8}$$

Modified pulse method (MPM)

Thermal diffusivity in this method is determined based on the measurement of the temperature difference between the sample's front (x = 0) and back (x = l) surface Figure 2b. Temperature changes on the extreme surfaces of the tested sample and their differences along with the values characteristic for these changes. The error made as a result of replacing the exact solution of the series of the temperature difference between the extreme surfaces of the sample with the temperature difference for the first term of this series is shown in Figure 2a and it is less than 1% for $t/\tau \cong 0.58$.

To determine the thermal diffusivity a, based on the recorded waveforms of changes in temperature differences $\Delta\Theta'(t)$, between the front and back surfaces of the tested sample, after a laser shot at its front surface, the characteristic time τ and the temperature increase Θ_∞ of the sample should be determined after of the transition process and is determined from the dependence:

$$\tau=(t_2-t_1)\left[ln\frac{\Delta\Theta'(t_1)}{\Delta\Theta'(t_2)}\right]^{-1} \tag{9}$$

where: t_1 – initial temporal range of the approximation;
t_2 – final temporal range of approximation;
$\Delta\Theta$ – temperature differences.

On the basis of the experimentally determined values of the characteristic time τ and the thickness of the sample l, the thermal diffusivity a of the material of the tested sample is determined, from the dependence which has the following form:

$$a=\frac{l^2}{\pi^2\tau} \tag{10}$$

As a criterion for the correct determination of the characteristic time τ, and thus the thermal diffusivity a, during the identification process, the

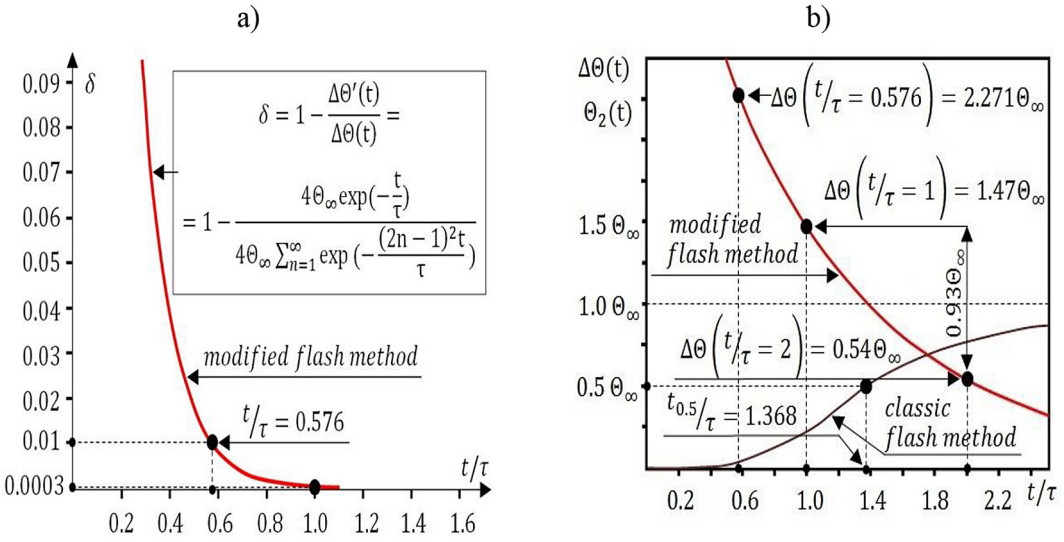

Fig. 2. Error made by replacing $\Delta\Theta(t)$ by $\Delta\Theta_{n=1}(t)$, temperature rise curves and change of temperature difference on the sample to determine thermal diffusivity by pulse method [28]

minimum mean square error between the recorded waveform and its theoretical form obtained from solving this problem, i.e., between the measured and theoretical temperature difference on the extreme surfaces of the tested sample, is assumed. This parameter is minimized in the range t_1,÷ t_2 by shifting the signal on the ordinate axis. The process stops when a satisfactory agreement is reached between the theoretical curve $\Delta\Theta(t)$ and the experimentally recorded $\Delta\Theta'(t)$ [26, 28, 30].

Determination of the Seebeck coefficient of the differential thermocouple

During the experiment, temperature measurements T_0, $\Theta_2(t)$ and $\Delta\Theta(t)$ were made with thermocouples. In the case of T_0 and $\Theta_2(t)$ it was a Fe-CuNi thermocouple. On the other hand, the temperature difference $\Delta\Theta(t)$ on the extreme surfaces of the tested sample was measured with a differential thermocouple, formed by two series-connected junctions "CuNi thermoelectrode–sample front surface" and "rear surface of the sample – CuNi thermoelectrode". The schematic diagram of the method of carrying out these measurements is shown in Figure 3. Temperature measurements T_0 and $\Theta_2(t)$ are easy to carry out because the $k(T)$ characteristic of the Fe-CuNi thermocouple is known. However, it is a rule that the $k_t(T)$ characteristic of the thermocouple "CuNi - material of the tested sample" is not known. Without the known $k_t(T)$ characteristic, it is not possible to determine the value of the ΔT interval by averaging the determined value $a(T)$.

This problem was solved by the simultaneous measurement of $E_2(T)$ and $E(T)$ and in both

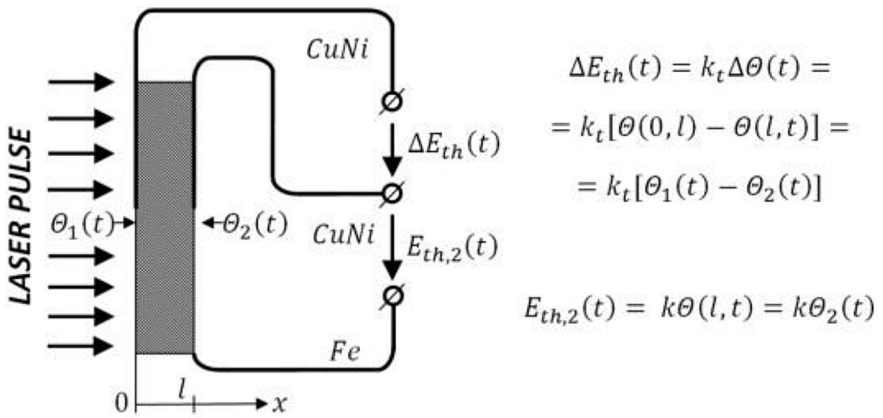

Fig. 3. Principle of the temperature measurement $\Theta_2(t)$ [$=T_2(t\leq 0)-T_0$] and the difference of temperature $\Delta\Theta(t)$ [$=\Theta_1(t)-\Theta_2(t)$] between the extreme surfaces of the sample: k_t – the constant coefficient of the thermocouple "CuNi–the material of the investigated sample"; k – the constant coefficient of the thermocouple "Fe - CuNi"[30]

cases the Thermo-Electric Force, in the assumed ranges of temperature changes, are linear functions of $\Theta_2(t)$ and $\Delta\Theta(t)$, respectively. In both cases, after the heat transfer process in the sample has been established. Hence, the following equation is obtained:

$$k_t = 0{,}25k\frac{\Delta E_{n=1}(t=0)}{E_2(t\to\infty)} \tag{11}$$

where: k_t – the constant coefficient of the thermocouple "CuNi - the material of the investigated sample".

During the measurements (Fig. 3), the signals $E_{th,2}(t)$ and $\Delta E_{th,2}(t)$ were amplified, and the amplification factor in both cases was K = 10000.

METROLOGICAL CONDITIONS

The correct determination of thermal diffusivity by the modified pulse method requires meeting several requirements imposed both by the heat transfer model on which the given method is based and by the measurement data acquisition and processing system. The most important of them are listed below:

- Starting from the generation of a surface heat source, the condition of the adiabaticity of the sample must be met on the front surface. It is met when the measurement is carried out in a vacuum ($p \leq 2 \cdot 10^{-4}$ Pa) and the heat dissipation through the elements fixing the sample in the furnace is minimal (conical ceramic elements were used).
- Fulfillment of the condition of one-dimensionality of heat exchange in the sample is ensured by the appropriate selection of the ratio of its diameter d to thickness l, and its value should be greater than $d/l \geq 6$. Also, the local values of the surface density of the created heat source should be the same.
- To eliminate the influence of the duration of the laser radiation pulse on the course of changes in the measurement signal $\Delta\Theta(t)$, the limit value on the time axis should be $t = t_g = t_0 + 0.2\tau$.
- An unfavorable factor affecting the correctness of determining the thermal diffusivity $a(T)$ by the modified pulse method is the possibility of initial temperature polarization of the tested sample (i.e. if $T(x,t=0) \neq T_0 = idem$ just before the formation of a surface heat source on the front surface). This type of phenomenon can occur in a sample when its extreme surfaces are asymmetrically heated in a vacuum furnace. In practice, if the condition $\Delta\Theta(t<0) \neq \Delta\Theta(t=7\tau)$ is met, it can be assumed that there is no initial polarization of the sample.
- The influence of the measurement system noise depends on the frequency response and the spectral density of the noise generated in the signal source and the measurement amplifier. Noise generated in the signal source –in this case in thermocouples –can be neglected due to the negligible value of their resistance (a few Ω). To minimize the noise of the measurement system, the frequency response of the amplifier should be limited to a value that does not cause significant distortion of the signal. Limiting the frequency response distorts the signal that grows rapidly (immediately after the laser shot). However, since only a portion of the waveform can be used for the calculation (for $t \geq 0.58\tau$), the distortion of the initial portion of the waveform does not affect the measurement result.
- From the point of view of the experiment, the characteristic time of the thermoelectrode materials, welded to the extreme surfaces of the samples, is also important. In this case, the materials of the test sample are Ni, and thermoelectrodes of constantan (CuNi) and iron (Fe) were used to measure the temperature (Fig. 5). Taking into account that: ≅ 50 μm $a_{CuNi} = 11.4 \cdot 10^{-6}$ m²/s, and $a_{Fe} = 22.2 \cdot 10^{-6}$ m²/s received: τ_{CuNi} = 22.3 μs and τ_{Fe} = 11.43 μs. That is, the time $t_i \cong 7\tau_i$, necessary to equalize the temperature in the volume of thermoelectrodes made of constantan and iron is in both cases at least 7 times shorter than the conventional duration of the laser pulse $t_i \cong 1$ ms.
- During the experiment, the temperature interval of averaging the thermal diffusivity value, determined based on the course of the $\Delta\Theta(t)$ curve, can be influenced in two ways:
  - moving the interval (t_2-t_1) of determining the characteristic time t to the right on the time axis;
  - by the surface density of the beam of the radiation flux incident on the test sample generated by the laser. The temperature range within which the averaging of the thermal diffusivity values takes place is:

$$[\bar{T} - (\Delta T)_2] \div [\bar{T} - (\Delta T)_1] \quad (12)$$

wherein: $\bar{T} = T_0 + \Theta_\infty$;

$\Delta T_1 = [T_0 + \Theta_1(t)] - \bar{T} = \Theta_1(t) - \Theta_\infty$

and $\Delta T_2 = \bar{T} - [T_0 + \Theta_1(t)] = \Theta_\infty - \Theta_2(t)$.

Where possible, the value $\Delta T = T_1 - T_2$ should be chosen in such a way that the condition is met $\Delta T = \Delta T_1 - \Delta T_2$ (Fig.2), then:

$$\bar{T} \pm 0.5\Delta T = (T_0 + \Theta_\infty) \pm 0.5\Delta T \quad (13)$$

where: T – Temperature;

T_0 –Thermostating temperature;

$\bar{T}$ – Average temperature.

- In the range of temperature changes higher than 400 K, an important factor was the consideration of heat losses by the tested sample.

EXPERIMENTAL RESEARCH

The thermocouple wires were attached to a sample with a thickness of l = 1.43 mm Figure 4a. The test sample, which is placed on a special boom in the central zone of the vacuum furnace, is shown in Figure 4b. The special structure of the boom and the created vacuum is designed to

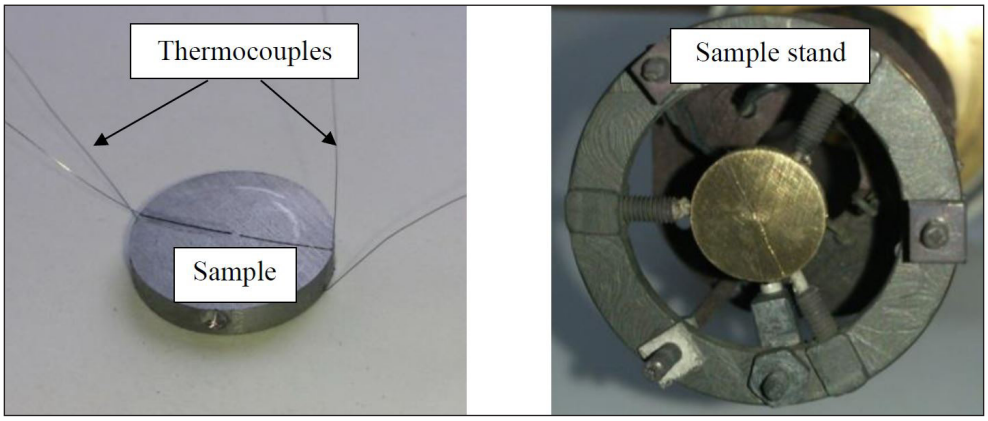

Fig. 4. The test sample and the same sample fixed in the support before being placed in the vacuum oven

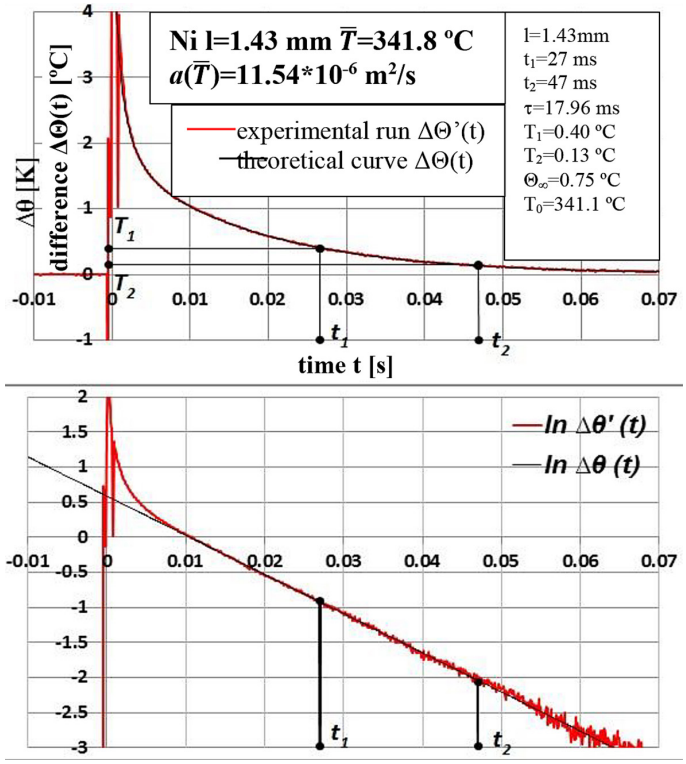

Fig. 5. An example of the final printout of the process of processing measurement data of thermal diffusivity of a nickel sample (Ni 999) with a thickness of l = 1.43 mm, at a temperature T_0 = 341.1 °C

minimize heat loss from the sample to the environment by conduction and convection.

Examples of studies on the thermal diffusivity of nickel 999 for the sampling temperature in the vicinity of the Curie point.

Following the procedure described earlier and observing the metrological conditions that determine the correct conduct of the experiment specified in chapter "Metrological conditions…", the thermal diffusivity was determined from the experimental run at the set temperature of thermostating, with the values $T_0 = 341.1$ °C of a nickel sample with a thickness of $l = 1.43$ mm (Fig. 5). Also, for this measurement $a(T) = T_0 + \Theta_\infty$), corresponding to a discrete value of the thermostating temperature $T = T_0 + \Theta_\infty$, a discrete value of the Seebeck coefficient was determined $k_{T=T0}$.

Sample final printouts of the measurement data processing process for determining thermal diffusivity are shown in Figure 5 (Modified method) and Figure 6 (Classic method). The method of determining the Seebeck coefficient is shown in Figure 7 with the most important values necessary for its calculation.

In addition, the most important parameter values identified were tabulated and presented in Table 1. Different values of thermal diffusivity can be observed for a given material at the

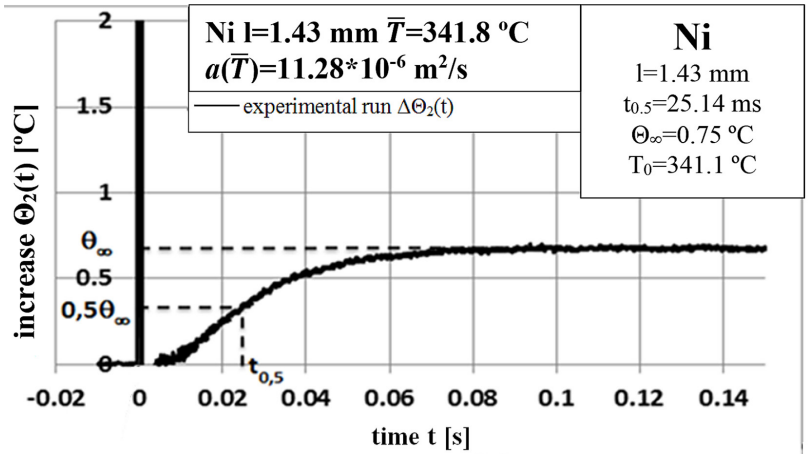

Fig. 6. Typical record of the final stage of numerical processing of the recorded temperature changes $\Theta(l,t)$ on the back surface of a nickel sample, after a laser shot at its front surface, during the determination of the thermal diffusivity of the sample using the classic (Parker) method

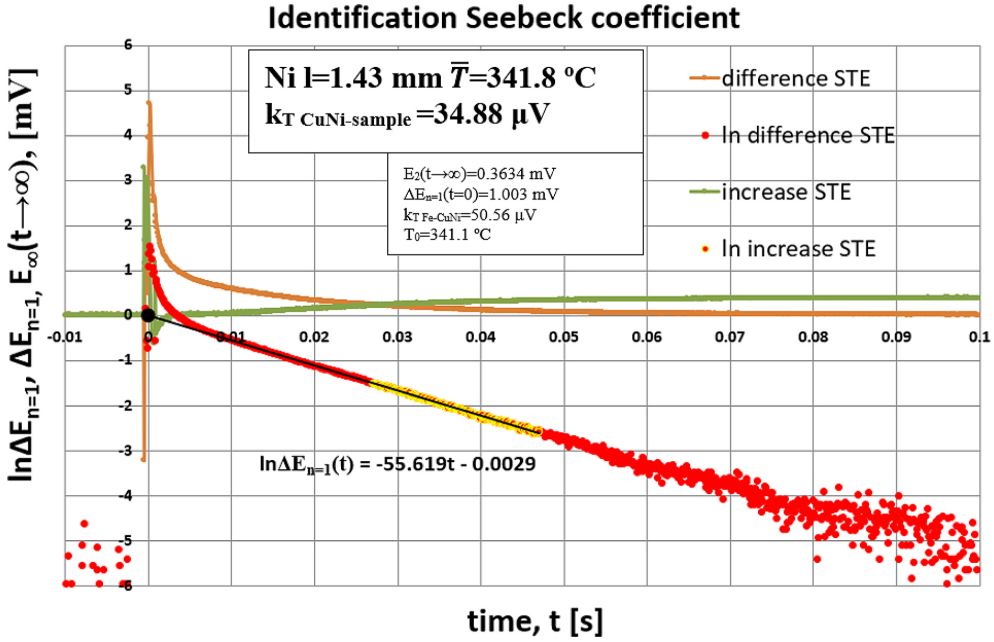

Fig. 7. Final printout of the experimental data based on which the Seebeck coefficient k_T was determined "CuNi–material of the tested sample"

Table 1. The most important parameters identified from the experimental run

No.	Parameter [unit]	Classic method	Modified method (MPM)
1	$t_{0.5}/\tau$ [ms]	25.14	17.96
2	$\bar{T}$ [°C]	342.6±1.5	341.8±0.37
3	$a(\bar{T})$ [m²/s]	11.28	11.54
Parameters for calculating the Seebeck coefficient k_T			
4	$E_2(t\rightarrow\infty)$ [mV]	0.3634	
5	$\Delta E_{n=1}(t=0)$ [mV]	1.003	
6	$k_{TFe\text{-}CuNi}$ [μV]	50.56	
$k_{T\ CuNi\text{-}sample}$ = 34.88 [μV]			

same temperature, determined by two methods in one measurement. This difference is about 2.2%, partly related to the different temperature ranges of thermal diffusivity averaging in these methods.

RESULTS

The numerical model was developed and numerical simulations were carried out in the COMSOL 3.5a environment by COMSOL MULTIPHISICS. The heat transfer was analyzed using the Heat transfer module. In this module, the physical process of heat conduction was simulated.

The following simplifications were introduced in the numerical analysis:

- in the heat transfer model, the condition of adiabaticity of the tested sample was assumed (during experimental tests, the vacuum is about 10^{-5} mbar) without any heat loss on the sample's fastening elements,
- the surface heat source was generated with an even distribution of thermal energy on the front surface and with the duration of the pulse equal to 1ms,
- the heat losses from the surface of the sample by radiation were not taken into account (however, the error that is made when determining the thermal diffusivity on this account at the set temperature of thermostating equal to 341 °C is less than 0.03 [26],
- the entered thermophysical values of the materials are the values at the set thermostatic temperature based on the material base MPDB v 7.49 [31].

The thermophysical properties of the tested sample and the most important values of the simulation of the numerical model were adopted based on scientific periodicals published in the literature (collected in the MPDB v 7.49 database) and summarized in Table 2.

Following the procedure described earlier and the procedure described in the experimental example and with the previously mentioned simplifying assumptions introduced during the numerical simulation, the values of thermal diffusivity and the Seebeck coefficient at the set thermostating temperature were determined, with the values $T_0 = 341.1$ °C of a nickel sample with a thickness of l = 1.43 mm. The simulation was carried out with a different number of nodal points, and the values of the identified thermal diffusivity parameter as well as the half-time and characteristic time are tabulated below.

Assuming that the material is homogeneous, and that the experimental tests were carried out

Table 2. Properties of the tested material and simulation parameters

No.	Thermophysical Parameter	Parameter[unit]	Value entered into COMSOL
1	Density	ρ [kg/m³]	8774.4
2	Heat capacity at constant pressure	c_p [J/kg/K]	623.37
3	Thermal conductivity	λ [W/m/K]	64.782
4	Time	t [ms]	100
5	Thickness	l [mm]	1.43
6	Diameter	φ [mm]	12
7	Temperature	T_0 [°C]	341
8	Inward heat flux	[W/m²]	$6\cdot10^6$

for axially symmetrical samples, the model was assumed to have isothermal edges on the outer sides, and the laser pulse was simulated by releasing energy onto the bottom surface. The reading took place under ideal conditions in which no additional well-conductive layers were required. Geometric models were created in the manner previously described, and with test parameter settings as below:

1. The subdomain settings were as follows:
   - General equation of heat transfer used in the model in Comsol Multiphysics:

$$\rho c_p \frac{\partial T}{\partial t} + \nabla(-k\nabla T) = 0 \tag{14}$$

   - Thermophysical properties of the tested material (Table 2).
   - Element settings for temperature: Lagrange–Quadratic.
2. The boundary settings were as follows – all planes were aligned symmetrically except for the bottom plane, where a laser pulse of less than 1 ms with an inward heat flux of $6 \cdot 10^6$ W/m^2 was simulated (Fig 8).

Numerical tests were carried out for one model with pre-determined boundary and starting conditions but for 5 different degrees of density of computational nodes. The temperature waveform from the opposite surface to the surface of heat

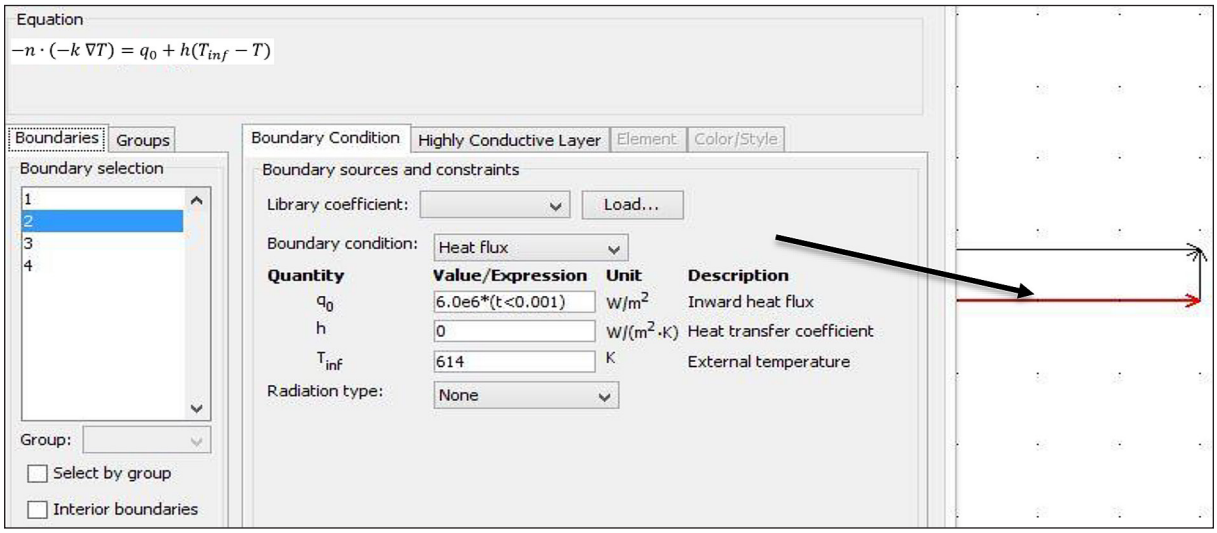

Fig. 8. Setting the boundary conditions for an exemplary geometric model

Table 3. Values of the identified thermal diffusivity parameter for the classic and modified method with various use of meshing during the simulation

No.	The number of COMSOL nodes	Parameter[unit]	Classic method	Modified method (MPM)
1	64	$t_{0.5}/\tau$ [ms]	24.7	17.34
2		$a(\bar{T})$ [m^2/s]	11.48	11.95
1	254	$t_{0.5}/\tau$ [ms]	24.36	17.48
2		$a(\bar{T})$ [m^2/s]	11.63	11.85
1	1054	$t_{0.5}/\tau$ [ms]	24.35	17.49
2		$a(\bar{T})$ [m^2/s]	11.64	11.84
1	4224	$t_{0.5}/\tau$ [ms]	24.32	17.49
2		$a(\bar{T})$ [m^2/s]	11.65	11.84
1	16896	$t_{0.5}/\tau$ [ms]	24.30	17.49
2		$a(\bar{T})$ [m^2/s]	11.66	11.84
Identification of the Seebeck coefficient k_T				
4	$min \sum_{i=100}^{i=900} [\Delta\Theta(t_i) - \widehat{\Delta\Theta}(t_i)]^2$		0.1277	
$k_{T\ CuNi\text{-}sample}$=34.26 [μV]				

drying was read at 0.0001 s. Linear system solver "Direct (UMFPACK)" was used. Figure 9a shows the dependence of the thermal diffusivity value on the number of nodal points.

Computational grid settings

A calculation grid with triangular elements was used (Fig. 9b). It is reasonable to introduce nodal points in the number of at least 256 (in Fig. 9b), for the number of points = 4224 due to the stability of the solution to the problem of heat conduction during the simulation. Calculations of the temperature field for the introduced numerical model with previous assumptions confirm that the temperature difference between the extreme surfaces of the sample after 0.1 seconds is about 0.01 °C and during the experiment 0.012 °C, which is shown in Figure 9b (temperature field).

The Seebeck coefficient was determined based on fitting the experimental curve to the simulation curve of the change in the temperature difference of the extreme surfaces of the sample. This identification was possible to determine from the known course of the thermoelectric force difference between the extreme surfaces of the tested sample for the CuNi-sample thermocouple and the simulation course of the temperature difference. The approximation interval was determined from about 0.6 τ to 90 ms (where τ ≈ 17 ms for a given experimental run). This was caused by the desire to avoid adjusting the beginning of the experimental run, where there may be disturbances in the uneven distribution of laser radiation energy on the front surface of the sample. The Seebeck coefficient of 34.26 μV was determined and the waveform fit for this value is shown in Figure 10b.

The values of the Seebeck coefficient were determined using the analytical method based on the experimental run as well as the second method supported by simulation. The difference between these values from the two methods is

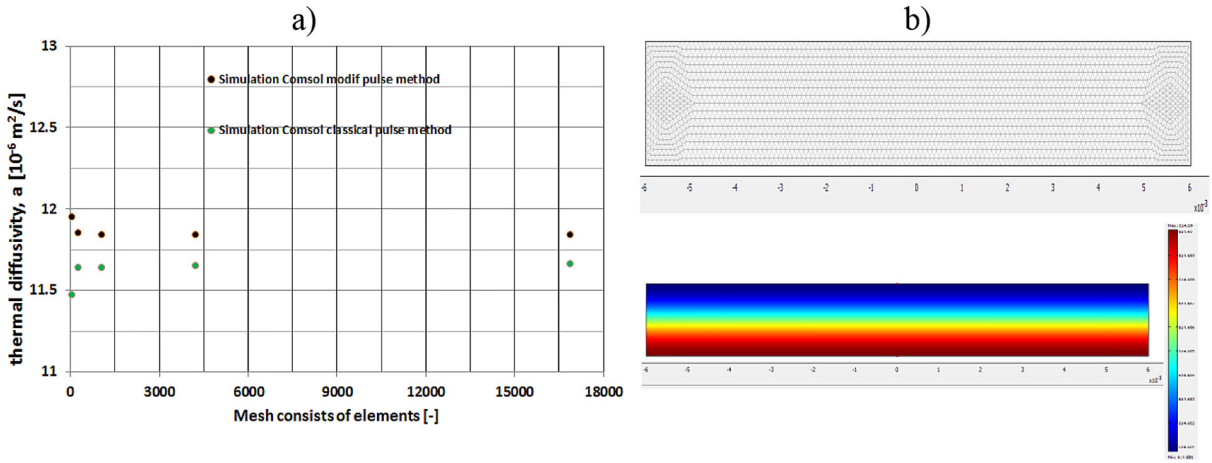

Fig. 9. a) The dependence of thermal diffusivity determined by two methods as a function of the number of points of the numerical grid, b) temperature field and grid in the COMSOL software

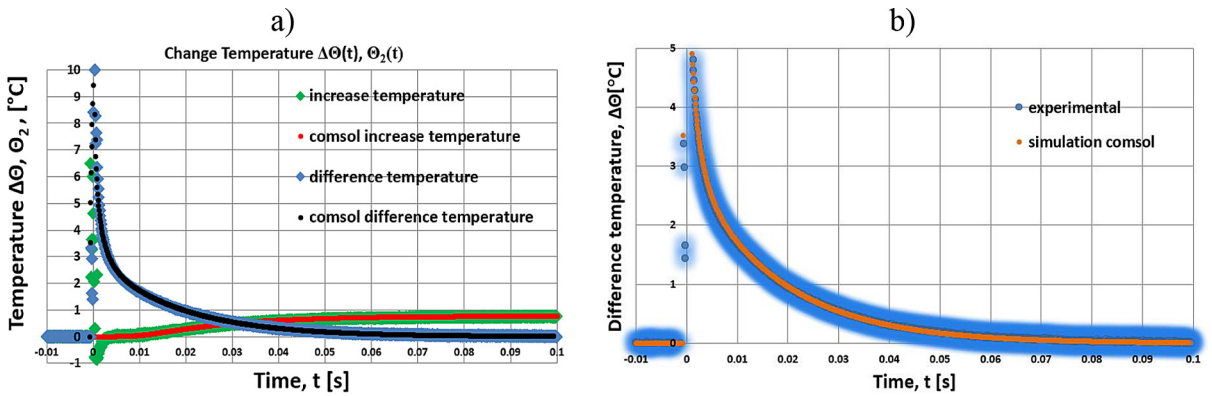

Fig. 10. a) Visualization of the change in the temperature difference between the extreme surfaces of the sample and the temperature increase on the back surface after a laser shot at the front surface from the experimental and numerical run; b) temperature distribution inside the sample after 0.1 s and calculation grid b)

about 1.8%. Owing to such precise identification of this coefficient, it is possible to precisely determine the thermal diffusivity averaging range. Figure 10 presents the values of thermal diffusivity, using the previously presented assumptions and set values necessary for identification, in relation to the set based on the Cindas and MPDB databases [31]. The Cindas material base is based on the measurement of thermal diffusivity using the Ångstream method, therefore a small number of points on the characteristics, the MPDB v 7.49 base is based on measurements of intermediate thermophysical values of materials, and the value of thermal diffusivity is determined based on the relationship $a = \lambda/\rho c_p$, where: λ – thermal conductivity, ρ – Density. When declaring the values of thermophysical parameters of nickel, MPDB was used and for these values, the value of thermal diffusivity was determined using two methods. Various numbers of nodal points were generated in the computational grids (discussed earlier); however, with very large numbers of these points, the thermal diffusivity value stabilizes at the level of $11.66 \cdot 10^{-6}$ m^2/s for the classic method and $11.85 \cdot 10^{-6}$ m^2/s for the modified method, as shown in Figure 11.

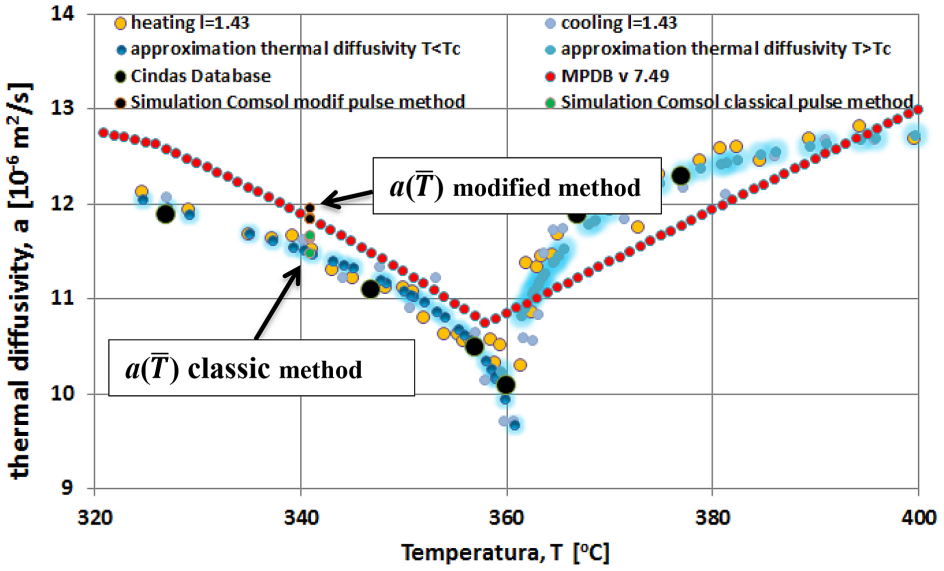

Fig. 11. Comparison of the thermal diffusivity of nickel l = 1.43 mm at T_0 = 341.1 °C obtained during the simulation with the values from the characteristics in the range of 300 – 400 °C obtained using the modified pulse method from experimental runs

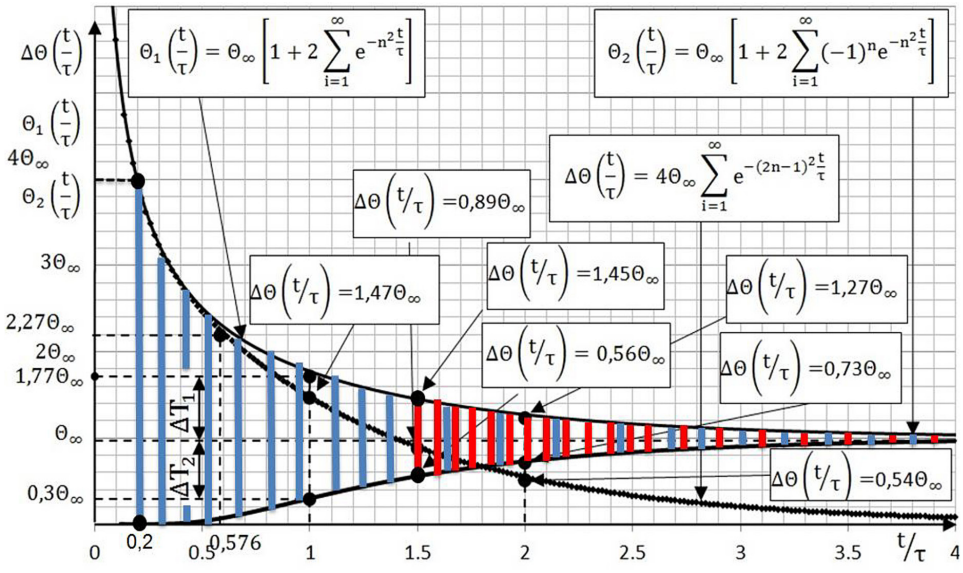

Fig. 12. Temperature changes on the boundary surfaces of the investigated specimen and the difference between them with the values characteristic of those changes

Having measured only the difference of thermoelectric forces on the extreme surfaces of the sample and simulation tests, the Seebeck coefficient necessary to determine the thermal diffusivity averaging temperature can be clearly determined.

When carrying out numerical simulations, it is also important, despite such a simple model, to select the appropriate number of nodal points, because, as shown in Figure 9, it is of reasonable importance. For a detailed discussion of the issue, the above work presents the procedure for determining thermal diffusivity and the exact temperature range of diffusivity averaging. Figure 11 shows the full temperature characteristics of this parameter and the value of the thermostating temperature was chosen so that its value was before the second type phase transition temperature. This is of significant metrological importance due to the dynamics of changes in thermal diffusivity and the related measurement problems, which is noticeable in significant discrepancies in determining thermal diffusivity in the immediate vicinity of the Curie point.

The above work presents the results of the numerical analysis of heat transfer for nickel and the determination of thermal diffusivity for this material by using both classic and modified methods. The results above were compared with the values obtained experimentally. When assessing the analysis, attention should be paid to discrepancies in the results of the same parameter from one parallel measurement, both numerically and experimentally, and this may be primarily due to the fact that the range of averaging thermal diffusivity determined by the classic method is much wider and ranges from T_0 to $T_0 + 4\Theta_\infty$ compared to the modified method where this range varies from $T_0 + 0.56\Theta_\infty$ to $T_0 + 1.44\Theta_\infty$, which is shown and marked in Figure12.

CONCLUSIONS

Due to the complexity of the problem, it is planned to repeat the measurements at temperatures slightly lower than the second-order phase transition temperature, so that the averaging temperature range covers both the steam and the ferromagnet during one measurement.

The heat transfer model used in the classic Parker method was subsequently used by other authors in various variations. Among other things, it was also used in the modified pulse method, the general outline of which is presented in this paper.

Using the developed and experimentally tested modified pulse method of diffusivity testing $a(T)$ of solids, it is possible to determine the values of this quantity in the temperature averaging range of less than 1 K and the estimated measurement error of less than 3%. In addition, a numerical simulation was carried out, based on which it is possible to determine the above coefficient using both the classic and modified methods. Significant discrepancies can be observed between the two methods resulting from a large change in thermal diffusivity as a function of temperature in the immediate vicinity of the Curie point.

The differences obtained between the values determined experimentally and numerically using the inverse problem are 3.3% for the classical method and 3.5% for the method modified in relation to the values obtained experimentally, respectively.

However, the influence of the number of computing nodes had a smaller impact and amounted to only 1.1% for the values obtained with 66 nodes and the values obtained with almost 17 thousand nodes. Owing to this analysis, the authors were able to present a combination of numerical and experimental research as well as present the methodological conditions of the study. In the next stage of numerical research, it is necessary to take into account the dependence of individual parameters as a function of temperature, which at the same time complicates the solution of the inverse problem, especially near the Curie point where the parameters change significantly with a small increase in temperature in the sample.

REFERENCES

1. Terpiłowski J., Jóźwiak S., Woroniak G., Szczepaniak R. Thermal Diffusivity Characteristics of the IN718 Alloy Tested with the Modified Pulse Method. Materials 2022; 15: 7881.
2. Su Y. Modelling and Characteristic Study of Thin Film Based Biosensor Based on COMSOL. Hindawi Publishing Corporation Mathematical Problems in Engineering 2014; 581063.
3. Singh S., Saha A.K. Numerical study of flow and heat transfer during a high-speed micro-drop impact on thin liquid films. International Journal of Heat and Fluid Flow 2021; 89.
4. Zhou J., Huang J., Liao J., Guo Y., Zhao Z., Liang H. Multi-field simulation and optimization of

SiNx:H thin-film deposition by large-size tubular LF-PECVD. Solar Energy 2021; 228: 575-585.

5. Yadav H.N.S.N., Kumar M., Kumar A., Das M.COMSOL simulation of microwave plasma polishing on different surfaces. Materials today: proceedings 2021; 45(6): 4803-4809.
6. Andreotta R., Ladani L., Brindley W. Finite element simulation of laser additive melting and solidification of Inconel 718 with experimentally tested thermal properties. Finite Elements in Analysis and Design 2017; 135: 36-43.
7. Zandi S., Saxena P., Razaghi M., Gorji N.E. Simulation of CZTSSe Thin-Film Solar Cells in COMSOL: Three-Dimensional Optical, Electrical, and Thermal Models. IEEE Journal of Photovoltaics, 2020; 10(5): 1503-1507.
8. Yantchev V., Turner P., Plessky V. COMSOL modelling of SAW Resonators. In: IEEE International Ultrasonics Symposium Proc. 2016.
9. Saxena P., Gorji N.E. COMSOL Simulation of Heat Distribution in Perovskite Solar Cells: Coupled Optical–Electrical–Thermal 3-D Analysis. IEEE Journal of Photovoltaics 2019; 9(6): 1693-1698.
10. Budakli M., Gambaryan-Roisman T., Stephan P. Gas-driven thin liquid films: Effect of interfacial shear on the film waviness and convective heat transfer. International Journal of Thermal Sciences 2019; 146.
11. Alrwashdeh S.S, Al-falahat A.M., Murtadha T.K. Effect of Turbocharger Compression Ratio on Performance of the Spark-Ignition Internal Combustion Engine. Emerging Science Journal 2022, 6(3), 482-492.
12. Zhoua L., Zhoua S., Dua X., Yang Y. Heat transfer characteristics of a binary thin liquid film in a microchannel with constant heat flux boundary condition. International Journal of Thermal Sciences 2018; 134: 612-621.
13. Alrwashdeh S.S., Ammari H., Madanat M.A., Al-Falahat A.M. The Effect of Heat Exchanger Design on Heat Transfer Rate and Temperature Distribution. Emerging Science Journal 2022, 6(1), 128-137.
14. Harsito C., Triyono T., Rovianto E. Analysis of Heat Potential in Solar Panels for Thermoelectric Generators using ANSYS Software. Civil Engineering Journal 2022, 8(7), 1328-1338.
15. Hemberger F., Ebert H.P., Fricke J. Determination of the Local Thermal Diffusivity of Inhomogeneous Samples by a Modified Laser-Flash Method. International Journal of Thermophysics 2007; 28: 1509–1521.
16. Szczepaniak R. Effect of Surface Topology on the Apparent Thermal Diffusivity of Thin Samples at LFA Measurements. Materials 2022; 15: 4755.
17. Pereira da Silva W., Pereira da Silva A., Matos de Souto L., Freire da Silva Junior A., Ferreira J.P. de L., Gomes J.P., de Melo Queiroz A.J. Determination of constant and variable thermal diffusivity of cashew pulp during heating: Experimentation, optimizations and simulations. Case Studies in Thermal Engineering 2022; 39: 102428.
18. Koyanagi T., Wang H., Mena J.D.A., Petrie C.M., Deck C.P., Kim W.J., Kim D., Sauder C., Braun J., Katoh Y. Thermal diffusivity and thermal conductivity of SiC composite tubes: the effects of microstructure and irradiation. Journal of Nuclear Materials 2021; 557: 153217.
19. Manta A., Gresil M., Soutis C. Transient conduction for thermal diffusivity simulation of a graphene/polymer and its full-field validation with image reconstruction. Composite Structures 2021; 256: 113141.
20. Lim K., Kim S., Chung M. Improvement of the thermal diffusivity measurement of thin samples by the flash method. Thermochimica Acta 2009; 494(1-2): 71-79.
21. Philipp A., Eichinger J.F., Aydin R.C. et al. The accuracy of laser flash analysis explored by finite element method and numerical fitting. Heat Mass Transfer 2020; 56: 811–823.
22. Ruffio E., Saury D., Petit D. Improvement and comparison of some estimators dedicated to thermal diffusivity estimation of orthotropic materials with the 3D-flash method. International Journal of Heat and Mass Transfer 2013; 64: 1064-1081.
23. Malinarič S., Bokes P. Impact of the Heat Source Model on Transient Methods of Conductivity and Diffusivity Measurement. International Journal of Thermophysics 2022; 43; 27.
24. García P., Mora, J., González del Val M., Carreño F., García de Blas F.J., Agüero A. Considering Thermal Diffusivity as a Design Factor in Multilayer Hybrid Ice Protection Systems. Coatings 2022, 12: 1952.
25. Beaufait R., Ammann S., FischerL. The Elephant Problem—Determining Bulk Thermal Diffusivity. Energies 2021, 14: 7444.
26. Szczepaniak R. Attempts to Identify the Curie Point Using a Modified Laser Flash Method, PhD. Thesis. Military University of Technology, 2014.
27. Parker W.J., Jenkins R.J., Butler C.P., Abbot G.L. Flash method of determining thermal diffusivity heat capacity and thermal conductivity. Journal of Applied Physics1961; 32: 1679-1684.
28. Terpiłowski J., Woroniak G., Szczepaniak R., Rudzki R.Metrological conditions for the research of thermal diffusivity of ferromagnetic alloys using the modified pulse method. Publishing House of the Rzeszów University of Technology, 2014.
29. Carslaw H.S., Jaeger I.C. Conduction of Heat in Solids, 2nd ed. Oxford University Press, 1986.
30. Terpiłowski J., Szczepaniak R., Woroniak G., Rudzki R. Adaptation of the modified pulse method for the determination of thermal diffusivity of solids in the vicinity of second-order phase transition points. Archives of Thermodynamics 2013; 34(2): 71-90.
31. Material Property Database. MPDB, v. 7.49. JAHM Software 1 nc, www.jahm.com; 2012.